Turkish Computational and Theoretical Chemistry

Turkish Comp Theo Chem (TC&TC)

Volume(Issue): 7(1) – Year: 2023 – Pages: 37-50

e-ISSN: 2602-3237

https://doi.org/10.33435/tcandtc.1102295

Received: 15.04.2022 ***Accepted:*** 15.06.2022 *Research Article*

Computational analysis using ADMET profiling, DFT calculations, and molecular docking of two anti-cancer drugs

Anaridha Saleem[a], Mohamed Imran Predhanekar[b], Khaja Mohideen Abbas[a], Salim Meeran Ismail[a], Shabeer Timiri Khudus[a, 1]

[a]The New College (Autonomous), Chennai – 600 014, Tamil Nadu, India.
[b]Islamiah College, Vaniyampadi, Tamil Nadu, India.

Abstract: U.S. FDA-approved anti-cancer drugs, namely ribociclib and copanlisib, used for treating breast cancer and follicular lymphoma, respectively, were chosen for computational study. Quantum chemical calculations via DFT and MP2 were used for energy optimization of the drugs. Chemical descriptor values for all the atoms were computed and compared using DFT and MP2 values. Herein we report the most reactive and stable atoms in the drugs. To describe the reactivity and stability of the drug molecules, Fukui functions were calculated. The drugs were docked against the epidermal growth factor receptor and cellular inhibitor of apoptosis protein-1 receptor to study the drug-protein interactions. The binding energy values before optimization and after optimization were found to be -11.21 and -14.41 kcal for copanlisib and -13.58 kcal and -29.08 kcal for ribociclib, respectively. Atoms O27 and O10 are reported to be the most reactive atom based on high softness values. Using SwissADME tool, the ADMET properties of the drugs were profiled. The results indicated good to moderate solubility and low to high absorption in the gastrointestinal tract. Predicted toxicity was class five for both anti-cancer drugs. The structural and bioactive properties of the drugs focused on in this study help evaluate the better reactivity patterns of anticancer medicines.

Keywords: Anti-cancer, ADMET, DFT, Molecular Docking, Fukui Function, HOMO-LUMO.

1. Introduction

Cancer is a complex and deadly disease characterized by uncontrolled cell proliferation. It is the second leading reason for death after cardiovascular disease [1]. Tumors are classified as benign and malignant. Benign tumors remain confined without invasion or metastasis. Surgical removal may cure it in most cases, and the patient generally survives. On the other hand, malignant tumors penetrate or infiltrate the neighboring tissues. Cancer is a general term used to describe malignant tumors. Cancer spreads to distant areas, where the malignant cells persist, cultivate, and invade again, unfortunately resulting in death [2].

Breast cancers are conceptualized using several characteristics. The gene receptor expression patterns, human epidermal growth factor receptor-2, and hormone receptors are some of the most common sporadic breast cancer subtypes [3,4]. Self-sufficiency of growth signals, metabolic reprogramming, evasion of apoptosis, limitless replicative potential, and evasion of immune recognition are some of the main hallmarks of the disease. Each effect alters some cellular activities which results in elevates cell proliferation, drops cell attrition, poor DNA repair, parenchymal dysregulation etc. [5].

Follicular lymphoma is a type of non-Hodgkin lymphoma caused by slow growth due to uncontrolled differentiation and expansion of lymphocytes. Lymphocytes that grow and proliferate uncontrollably can spread to other parts, including bone marrow, spleen, lymph nodes and develop tumour cells. The normal or modified cell functions of each human cell is preserved by signaling pathways by the canonical and non-

[1] Corresponding Authors
e-mail: shabeer@thenewcollege.edu.in

canonical components and intracellular signal networks [6]. The identification of the tumor microenvironment is accomplished by using molecular profiling that includes clinical diagnosis and tumour biomarking therapy [7].

Bioinformatics tools play an incredible and substantial role in the evolution of clinical research, examining terabytes of genomic data from tumor cells and germ-line genome and proteome profiles. Structure and ligand-based approaches are the most used methods in drug discovery. It is pivotal to use a computational approach to predict drug-targeted interactions. Molecular pathway studies illustrate canonical pathways and their perspectives in different cancers. Advanced technologies, such as molecular dynamics simulation, docking, structural and functional studies of protein, and QSAR have been adopted to evaluate the efficacy of small inhibitors of cancer-related biological molecules. [8-10].

Because of the above facts, we are interested in exploring the computational analysis of two anti-cancer drugs, viz ribociclib and copanlisib. In this study, we adopted in-silico approach to investigate the molecular dynamics, energy optimization, and molecular docking of the selected anti-cancer drugs. Further, we investigated the complete ADMET profiling of the drug molecules. This research work enlightens the mode of action and the possibility of improving the drugs' activities against cancer cells. The conclusions of this study could give an accurate and in-depth assessment of the drugs' putative intermolecular interactions and biological activities.

Density functional theory (DFT) has a significant effect on drug research and development. DFT can precisely represent biologically important chemical systems at a lower computing cost than other approaches, making it a widely used methodology [11-14]. Global and local reactivity parameters play a vital role in comprehending and predicting the chemical reactivity and other molecular properties. Electronegativity, chemical potential, hardness, softness, etc., are examples of global descriptors. Ionization potential, local softness, local polarizability, local hardness, molecular electrostatic potential, etc., comprise the local parameters. The data on these parameters help to describe the binding phenomena and partition.

Investigation of frontier molecular orbitals signifies molecular interactions that are noteworthy in understanding the molecular biology and biochemical functions of the drugs. The electron-donor property is governed by the highest occupied molecular orbitals (HOMO), while the electron-acceptor property is governed by the lowest unoccupied molecular orbitals (LUMO). The electron density measured using local reactivity descriptors specifies the positive reactive sites of the molecule, which is important for pharmaceutical drug design. The interrelated HOMO energy and ionization potential characterize the susceptibility of the molecule to electrophilic attack. Electron affinity is proportional to its LUMO energy, indicating that the molecule is susceptible to nucleophilic attack [15]. The energy gap between HOMO and LUMO is a prominent stability index.

As shown below, electron affinity (EA) and ionization potential (IP) are connected to HOMO and LUMO energies.

IP = -E(HOMO)
EA = -E(LUMO)
Electrophilicity (ω) = $\mu^2/2\eta$

Electronegativity ($\varkappa$) is the negative value of electronic chemical potential (μ). Chemical potential [16] is the tendency of electron flow from a region of higher to lower potential, until uniformity is achieved.

$$\mu = \left(\frac{\partial E}{\partial N}\right)\upsilon(r) = -\varkappa$$

$$-\mu = \frac{IP + EA}{2} \qquad = -\varkappa$$

Where E is the total electronic energy, (r) denotes the external electronic potential, N the number of electrons, and electrons in υ(r) feel due to nuclei. The equations above can calculate the numerical values of electronegativity and chemical potential.

The chemical hardness (η) [17] is the resistance of a molecule to utilize the electrons, which can be measured by,

$$\eta = \in_{HOMO} - \in_{LUMO}$$

The inverse of chemical hardness is the global softness, S [18]. The ability to retain the acquired electronic charge is called charge capacity.

Softness(S)=$S=1/2\eta=(\in_{LUMO}-\in_{HOMO})/2$
Local softness=Fukui function x global softness

The Fukui function along with DFT predicts the nucleophilic and electrophilic sites in a molecule.

For nucleophilic attack: $f_x^+ = q_x(N+1) - q_x(N)$
For electrophilic attack: $f_x^- = q_x(N) - q_x(N-1)$
For radical attack: $f_x^0 = 1/2[q_x(N+1) - q_x(N-1)]$

N is the number of electrons in the molecule [19-22]. N+1 is, therefore, an anion, with an electron added to the LUMO of the molecule. N-1 would be the cation that has an electron removed from the HOMO of the molecule. An atomic charge partitioning method, such as Mulliken population analysis, can condense these functions to the nuclei [23].
Time-dependent density functional theory (TD-DFT) was proposed by Runge and Gross thirty years ago. Casida developed comprehensive linear-response (LR) method for TD-DFT a decade later. As a technique for modeling the energies, characteristics of electronically excited states, and structures, TD-DFT has evolved in prominence [24].

2. Computational Method

The chemical structure of each drug was drawn in Chemsketch [25] and subjected to correction by using Avagadro software [26]. The Gamess input was created from these mechanics using Facio tools [27] and submitted to the GAMESS programme for final optimization using the 631G basis set at DFT (B3LYP) and MP2 levels. Autodock tools (version 1.5.6) and autodock docking programs (version 4.2.6) were used for molecular docking studies. The target protein structures were downloaded from the protein data bank (http://www.rcsb.org./pdb). Before and after DFT optimization of the drugs, molecular docking was done with the corresponding protein [28]. From autodock, the docking results were recorded as an extension file (.dlg). Based on the docking score, the pose with lowest energy was considered as the best binding mode. The visualization of docking conformations were done with Discovery Studio [29] and Pymol Viewer, and the four best poses for each drug molecule were tabulated in Table 5. SwissADME [30] and Protox-II [31] were used to complete the ADMET profiling of the drugs. Argus Lab [32] was used to obtain the molecular electrostatic potential map. Chemcraft [33] was used to complete molecular orbital calculations and evaluate local and global reactivity descriptors.

2.1 Selection of drugs

The two anti-cancer drugs, namely ribociclib and copanlisib, completed the clinical trials and approved by the Food and Drug Administration, US to treat breast cancer and follicular lymphoma, respectively, were selected for insilico analysis. Ribociclib (7-cyclopentyl-N,N-dimethyl-2-[(5-piperazine-1-ylpyridin-2-yl)amino]pyrrolo[2,3-d]pyrimidine -6-carbox-amide) is an anticancer medication reported to treat breast cancer, using CDK4 and CDK6 as its target receptors. [34]. It is a pyrolo-pyrimidine derivative that functions as an antineoplastic agent. In phase III clinical studies for breast cancer, the medicine revealed increased CDK4/6 specificity, with (IC50) values for cyclin D1/2/3-CDK6 of 10 nM. The drug also demonstrated antitumor activity in neuroblastoma, liposarcoma, rhabdomyosarcoma, and Ewing sarcoma xenografts. It inhibits RB phosphorylation and origins cell arrest of tumor cells [35]. This drug prevents cancer cell proliferation in G1phase by specifically inhibiting cyclin D1-CDK4 and cyclin D3-CDK6 complexes of the CDK target proteins [36]. Ribociclib has potential against other solid tumors in addition to breast cancer therapy.
Copanlisib (2-amino-N-{7-methoxy-8-[3-(4morpholinyl) propoxy]-2,3-dihydroimid-azo [1,2-c] quinazolin-5-yl}-5-pyrimidinecarboxamide) is a selective pan-class-1 phosphoin-ositide3-kinase (P13K) inhibitor approved on September 14, 2017, to treat various hematological and solid cancers. According to the findings of the phase-2 trial, the drug is used to cure patients with recurrent follicular lymphoma who have had at least two prior systemic therapies. The drug inhibits the phosphatidylinositol-3-kinase (P13K) p110 and p110 isoforms generated by malignant B cells. Apoptosis [37] promotes cell death and inhibits the differentiation of primary malignant B-cell lines. The drug demonstrated potent anti-tumor and pro-apoptotic effects [38] in a variety of tumour cell lines and xenograft models. With an acceptable toxicity profile [39], the drug is a safe and effective therapy choice for patients with

recurrent follicular lymphoma. In patients with highly pre-treated marginal zone lymphoma (MZL), small lymphotic lymphoma (SLL), and chronic lymphotic leukaemia (CLL), the drug is also effective as a single agent [40].

3. Results and discussion

3.1 ADME Profiling

A drug's pharmacokinetics and metabolic fate in the body are greatly affected by the physicochemical qualities. The predicted physicochemical and pharmacokinetic properties of the two drugs are tabulated in Table 1. Molecular weight less than 500 is one of the criteria of the Lipkinsi rule of five. The molecular weights of both drugs are found to be less than 500. Predicting topological polar surface area (TPSA) parameter is used to understand the passive molecular transport of drug molecules. The TPSA value must range between 71 Å² and 131 Å². The TPSA value of ribociclib (91.21 Å²) is within the optimum range, whereas for copanlisib, the value (142.01 Å²) is found to be a little higher. The high solubility promotes total absorption, whereas low solubility reduces drug absorption in the gastrointestinal system. If the log Kp (cm/s) is more negative, the skin permeant of the drug is considered to be less. Log Kp values are found to be within the optimal range of -8.0 to -10.0.

Table 1: Predicted Physiochemical and Pharmacokinetics properties of two drugs

S.No	Physicochemical Properties	Ribociclib	Copanlisib
1.	MW	434.54	480.52
2.	RB	6	8
3.	TPSA (Å²)	91.21	142.01
4.	ESOL CLASS	SOL	SOL
	Pharmacokinetic Properties		
5.	GIA	High	Low
6.	P-gp S	Yes	Yes
7.	BBBP	No	No
8.	Log Kp(cm/s)	-7.40	-9.00
9.	CYP1	No	No
10.	CYP2	Yes	Yes

MW- Molecular Weight, RB - Number of Rotatable bonds, TPSA – Topographic Polar Surface Area, Cons. Log P- Consensus. Log P, ESOL - Water Solubility, GIA – Gastro-Intestinal, Absorption, P-gp S - Permeability glycoprotein Substrate, BBB P- Blood-Brain Barrier Permeability, log Kp (cm/s) - Skin permeant, CYP1 - CYP2C9 inhibitor, CYP2 - CYP2D6 inhibitor.

3.2 BOILED-Egg Model

The Brain Or Intestinal EstimateD permeation (BOILED-egg) method is a graphical method for predicting passive human gastrointestinal absorption (GIA) and brain permeability. The yolk in the egg-shaped plot depicts physicochemical space with a high probability of brain penetration. The white area denotes physicochemical space with a high probability of passive absorption through the gastrointestinal tract [41].

In the outer grey zone, a molecule with predicted low absorption and limited brain permeability can be identified. As seen from the BOILED-Egg graph of two drugs presented in Figure 1, ribociclib is spotted in the white region describing its high gastrointestinal absorption, whereas copanlisib is spotted near the grey region could have low GIA. As a result, ribociclib may easily permeate the intestinal lining and thus available to the cell membrane. No BBB permeation for the two drugs with the peripheral target thus elucidates the absence of side effects in the central nervous system.

3.3 Lipophilicity and Drug-Likeness

The log P-value coefficient determines a drug's hydrophobic and hydrophilic properties whose optimal range is between –0.7 and +5.0. As a result, they are expected to have good permeability and oral absorption. The drugs were predicted to have good permeability and oral absorption based on their Log P values. Table 2 shows the lipophilicity, drug-likeness, and medicinal chemistry properties of the two drugs

3.4 Rule of Five by Lipinski

According to Lipinski's rule of five, a drug must violate none, or less than one, of the following four categories to be conceived as a prospective oral drug. The following are the criteria: Log P

(Octonal-Water partition coefficient) ≤5 number of hydrogen bond acceptors ≤10, number of hydrogen bond donors ≤5, molecular weight ≤500. The Abbot Bio Availability Score (BAS) is a semi-quantitative rule-based score based on the total charge, TPSA value, and violation of the Lipinski filter. According to Lipinski's rule of five, both the drugs under study fulfill all the four rules.

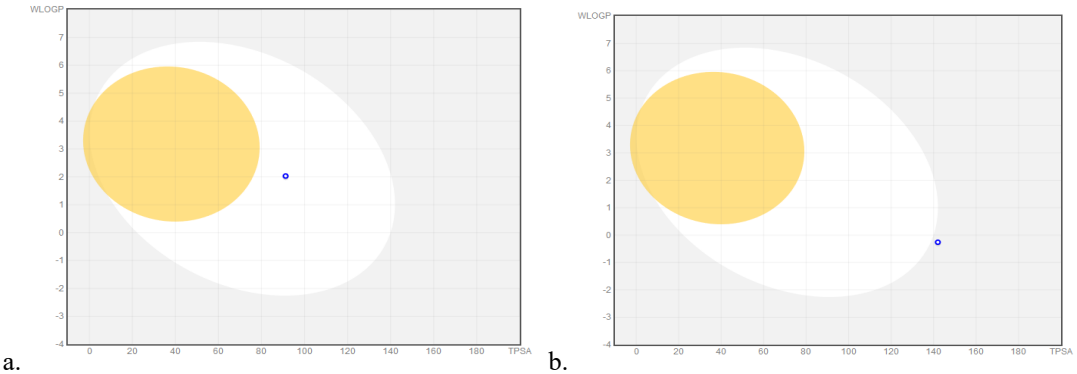

a. b.

Figure 1: BOILED-Egg representation of (a) Ribociclib and (b) Copanlisib

Table 2: Lipophilicity, Drug likeness, and Medicinal Chemistry properties of two drugs

S.No	Lipophilicity	Ribociclib	Copanlisib
1.	I LogP	3.34	3.40
2.	X Log P	2.19	0.33
3.	W LogP	2.03	0.26
4.	M LogP	1.38	-0.20
5.	Cons.Log P	2.01	0.99
	Druglikeness - No. of Violations		
6.	Lipinski	Yes	Yes
7.	Egan	Yes	No
8.	Ghose	No	No
9.	BAS	0.55	0.55
10.	Muegge Rule	Yes	Yes
11.	Veber	Yes	No
	Medicinal Chemistry		
12.	PAINS alert	0	0
13.	SA	3.47	3.91
14.	Brenk alert	0	0
15.	Lead likeness	No	No

Cons. LogP – Consensus LogP, L- Lipinski, E- Egan, G- Ghose, BAS- Bioavailability Score, M- Muegge Rule, V-Veber, SA– Synthetic Accessibility

3.5 Bioavailability Radar

The drug-likeness of a molecule can be determined using the bioavailability radar. The general parameters are: (a) SIZE (m.w): 150g/mol to 500g/mol; (b) Flexibility (Number of rotatable bonds): 0 to 9; (c) Polarity (TPSA): 20 Å² to 130 Å²; (d) Insaturation (Fraction Csp3): 0.25 to 1; (e) Lipophilicity (XLOGP3): -0.7 to +5.0; (f) Insolubility (Log S): 0 to 6;

For favorable physicochemical region of oral availability, the radar plot must be within in the pink zone. The bioavailability radar plots of two drugs are represented in Figure 2. The bioavailability radar plot of ribociclib is well within the pink zone and, hence, possesses good drug-likeness property. The radar plot of copanlisib is also within the pink region except for the polarity parameter, as the TPSA value (142.01Å²) is a little above the limit value of 130 Å². Hence, modifying

the polarity of the drug would results in improved druglikness of the molecule.

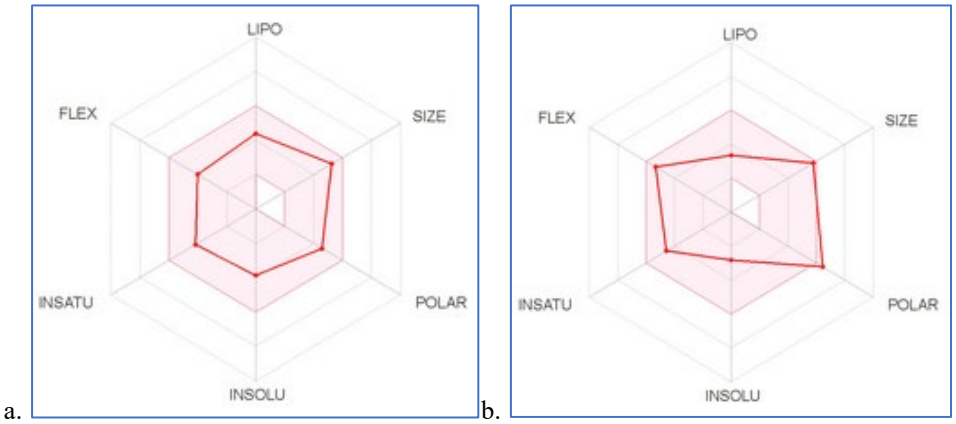

a. b.

Figure 2: Bioavailability Radar representation of (a) Ribociclib and (b) Copanlisib

Table 3: Descriptors from DFT and MP2 Calculation

Descriptor	Ribociclib (DFT) eV	Ribociclib (MP2) eV	Copanlisib (DFT) eV	Copanlisib (MP2) eV
HOMO Energy[#]	-4.8817	-7.2001	-5.3171	-7.7825
LUMO Energy[#]	-1.1809	2.3565	-1.5129	2.1714
Electronegativity	3.0313	2.4218	3.4150	2.8055
Softness	1.8503	4.7783	1.9020	4.9770
Hardness	-3.7008	-9.5566	-3.8042	-9.9539
Chemical Potential	-3.0313	-2.4218	-3.4150	-2.8055
Ionization Potential	4.8817	7.2001	5.3171	7.7825
Electron Affinity	1.1809	-2.3565	1.5129	-2.1714
Electrophilicity Index	-1.2415	-0.3068	-1.5328	-0.3953

[#] *Energy gap is computed as a difference* $\Delta E = E_{LUMO} - E_{HOMO}$ *in eV.*

3.6. Medicinal Chemistry:

The Synthetic Accessibility (SA) score is normalized between one (easy synthesis) and ten (complicated synthesis). If SA is less than four, the drug possesses good feasibility for synthesis [41]. The SA score of the drugs are 3.47 and 3.91; hence both drugs contain good feasibility to synthesize. The toxicity predicted from Protox-II software has shown that both the drugs belong to class-5 toxic level (significantly less harmful), and copanlisib was found to be immune-toxic.

3.7. Geometry optimization by DFT and MP2 method:

The energy optimization of the drug molecules and computation of global and local reactivity descriptors were carried out using DFT (B3LYP) and MP2 method with a 631G basis set. Figure 3 illustrates the energy-optimized structure of ribociclib and copanlisib in figure 4. Some significant parameters calculated from the DFT and MP2 optimized geometry of the drugs are tabulated in Table 3.

The energy differential between HOMO and LUMO is a significant stability index. The energy gap value of ribociclib (ΔE = 3.7008 eV) is quite lower than that of copanlisib (ΔE = 3.8042 eV). A lesser energy gap favors electronic transition, which leads to kinetic instability and more reactivity of the drug molecule. The chemical hardness [42,43] of a species specifies its resistance to the use of electrons, which may be estimated using the equation $\eta = \in_{HOMO} - \in_{LUMO}$. The hardness of the molecule indicates the chemical reactivity of the molecule. From table 3, ribociclib having a lesser softness value is expected to have good interactions with electrophilic sites.

To analyze the reactivity sites for nucleophilic and electrophilic attacks on the drug molecules, the electrostatic potential mapping was computed at the B3LYP/631G level using Argus lab software [44].

The electron density was classified in the following order: red > green > blue > pink > white.

The map shows that electron-deficient portions are detected around hydrogen atoms, whereas electron-rich regions are observed over nitrogen and oxygen atoms. Figure 5 demonstrates a graphical depiction of the chemically active regions, which are revealed to be ideal confirmation of biological activity in the title compounds [45]. As a result, the two-dimensional ligand-protein interactions and electrostatic potential map could be applied to quantify the hydrogen stability [46].

The electronic transition properties, which include the maximal excitation wavelength (λmax) and relative intensities (oscillator strengths, f) were calculated using time-dependent density functional theory (TD-DFT) using Chemcraft. From the computed results, ribociclib showed three bands, at 295.865 nm, 308.324 nm, and 379.965 nm, due to n→π* and π→π* transitions, respectively. Due to more unsaturated bonds, similar absorption bands were computed at a still higher wavelength for copanlsib at 334.781 nm, 343.889 nm, and 384.188 nm [47]. Absorption spectra of the drugs calculated by the TDDFT method are represented in figure 6.

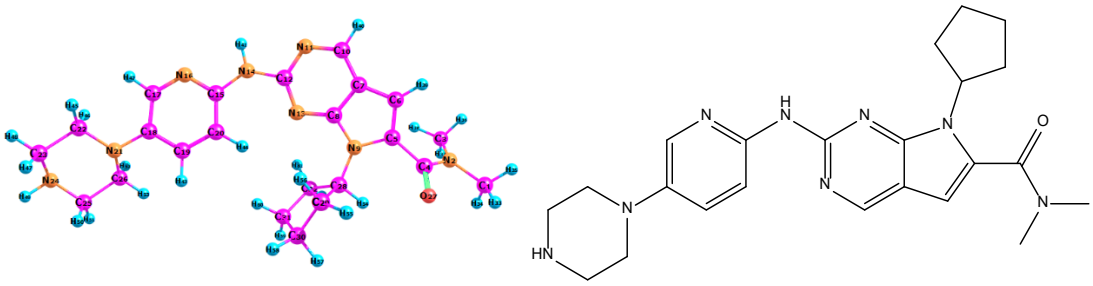

Figure 3: 6-31G DFT optimized structure of drug ribociclib

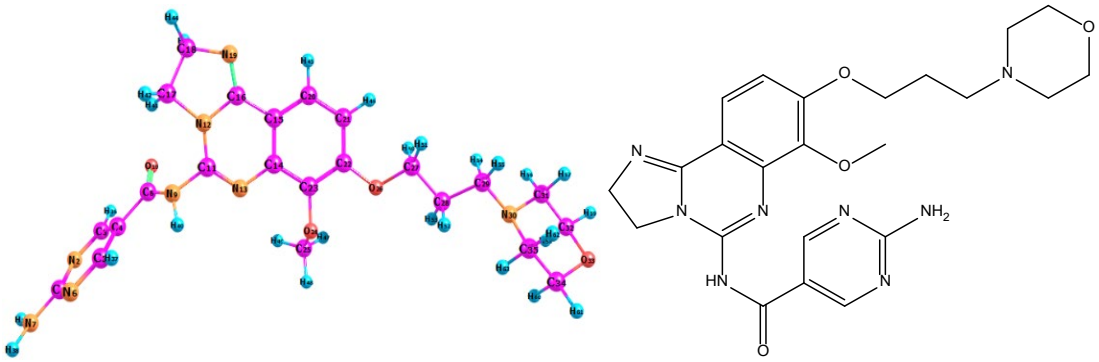

Figure 4: 6-31G DFT optimized structure of drug copanlisib

Table 4: Hardness table of a. Ribociclib (left) and b. Copanlisib (right)

S.No.	Atom	Hardness (DFT)	Hardness (MP2)	S. No.	Atom	Hardness (DFT)	Hardness (MP2)
1	N2	1.5254	4.5174	1	N2	1.7807	4.3219
2	N9	2.1357	5.5915	2	N6	1.7853	4.3498
3	N11	1.8555	4.5021	3	N7	2.8630	7.9422
4	N13	2.2023	5.2742	4	N9	2.6796	7.4733
5	N14	2.6975	7.3910	5	O10	1.9093	4.5738
6	N16	1.9196	4.6454	6	N12	2.0820	5.8777
7	N21	1.8985	5.1701	7	N13	2.2722	5.3422
8	N24	2.0432	5.8104	8	N19	1.9743	4.6265
9	O27	1.9484	4.7295	9	O24	1.9679	5.3422
				10	O26	1.9667	5.2994
				11	C28	1.1035	3.3036
				12	N30	1.5384	4.5529

13	O33	1.7750	5.0615

a. 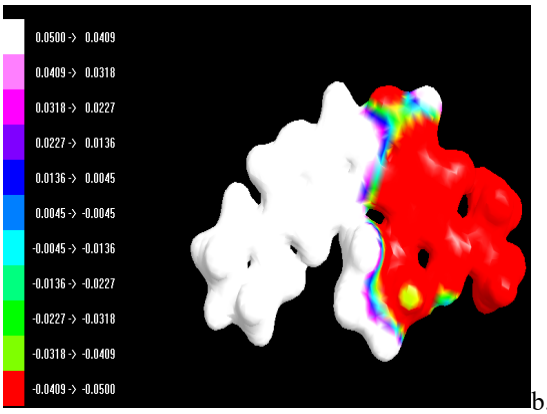

b. 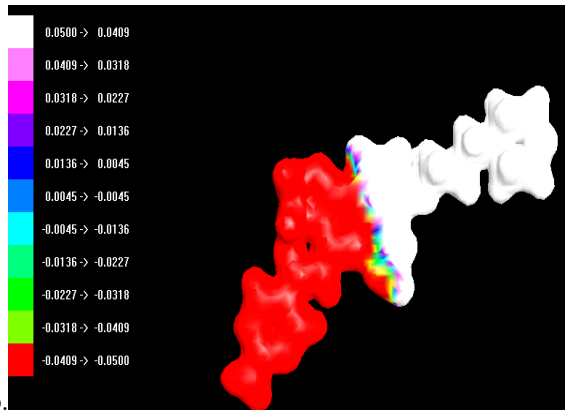

Figure 5: Molecular Electrostatic Potential map of (a) Ribociclib and (b) Copanlisib

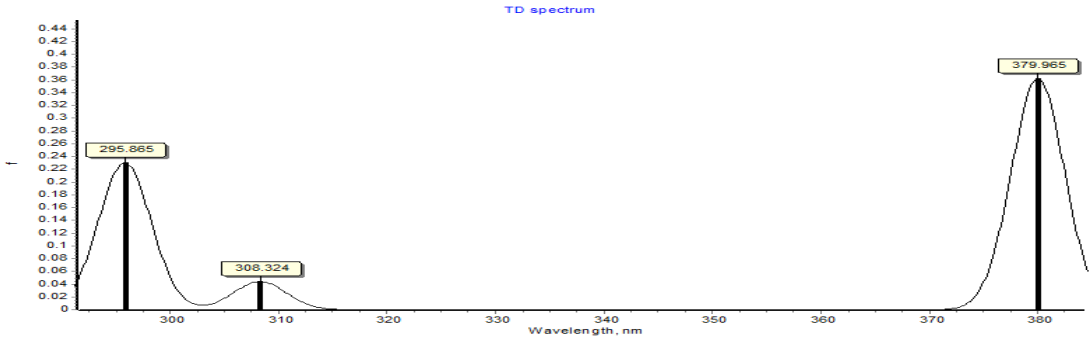

a.

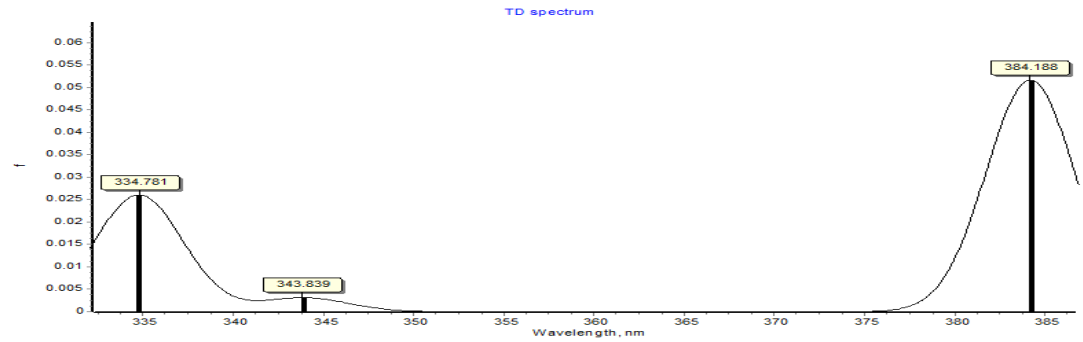

b.

Figure 6: TD-DFT spectra of (a) Ribociclib, (b) Copanlisib

3.8. Molecular Docking

Molecular docking via computational approach affords the most promising drug designing and discovery course. It is more economical, time-saving, and effective than conventional techniques [48, 49].

3.8.1. Protein target selection

As ribociclib was previously docked and reported with CDK4/6 and a few other kinases, the drug is docked with Epidermal Growth Factor Receptor (EGFR), resulting in good binding energy. Ribociclib with an aromatase inhibitor has been used for initial endocrine-based therapy. Because of its general function in signal transduction and oncogenesis, the EGFR family is one of the most studied receptor-protein-tyrosine kinase families [50]. The term cIAP1 (also known as BIRC2) refers to a human protein known as a cellular inhibitor of apoptosis protein-1. It is a member of the IAP protein family, including at least one BIR

(baculoviral IAP repeat) domain [51]. It is generally recognized that this protein has a substantial impact on the development of several malignancies. cIAP1 has a role in the development of osteosarcoma [52] and gastric cancer [53], among other diseases [54,55].

The drug ribociclib without optimization was initially docked with the macromolecule EGFR receptor (PDB ID: 3POY) using Autodock software. And secondly, the B3LYP/631G energy-optimized drug was docked with the protein receptor. The drug copansilib was docked into the active sites of the cIAP1 (PDB ID:3M1D) before and after optimization. The energy calculation of two drugs after docking analysis is tabulated in Table 5. A comparative study, before and after the energy optimization is reported. The binding affinities of Ribociclib before and after optimization are -13.58 kcal and -29.08 kcal respectively. From the docking visualization of ribociclib, the docked ligand is bound within the hydrophobic pocket consisting of amino acids viz. PRO 349, LEU 348, GLN 408, GLN 438, and HIS 409. Atoms N11, N24, and N16 were involved in hydrogen bond formation with water molecules at 2.5 Å,2.3 Å, and 3 Å, respectively. N14 forms two hydrogen bonds with two water molecules at 3 Å and 2.4 Å. Pyridine ring shows Pi-bond interaction with HIS 409 at 5.6 Å (figure 9).

Atoms O27 and N13 act as nucleophiles forming a hydrogen bond with GLN 384 at 1.9 Å and 2.3 Å, respectively. Since the atom N13 is present inside the ring, it was stabilized. Atom O27 shows more electronic effects due to conjugation and is more reactive.

Table 5: Docking results of ribociclib and copanlisib

S.No	Description	Ribociclib		Copanlisib	
		BO	AO	BO	AO
1.	Ligand Efficiency	-0.42	-0.91	-0.32	-0.41
2.	Inhibitory Constant	111.78	481.08	6.09	27.3
3.	Intermolecular Energy	-15.37	-30.57	-13.89	17.1
4.	vdW + H bond + dissolving energy	-1.16	-3.89	-2.29	-1.21
5.	Electrostatic Energy	-14.21	-26.69	-11.6	-15.89
6.	Total Internal Energy	39.44	-1.54	31.9	-0.81
7.	Torsional Energy	1.79	1.49	2.68	2.68
8.	Binding Energy	-13.58	-29.08	-11.21	-14.41

Note: BO: Before Optimization, AO: After Optimization. Energy values in kcal mol^{-1}

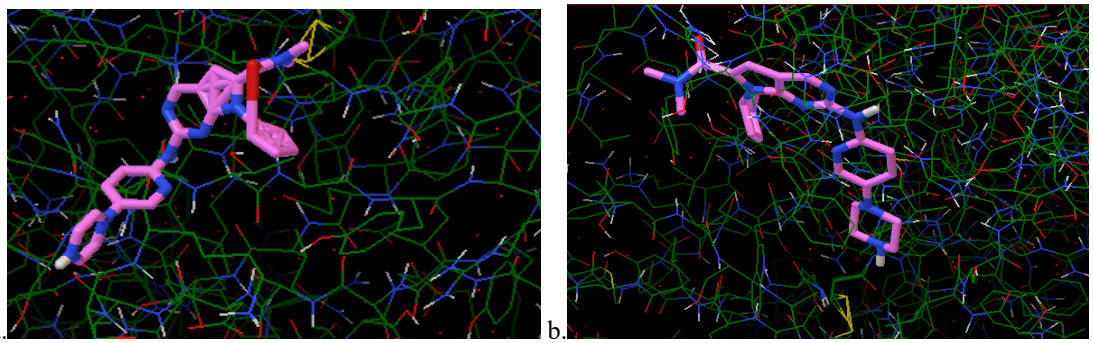

Figure 7: Docking of ribociclib (a) Ribociclib before optimization, (b) Ribociclib after optimization

a. b.

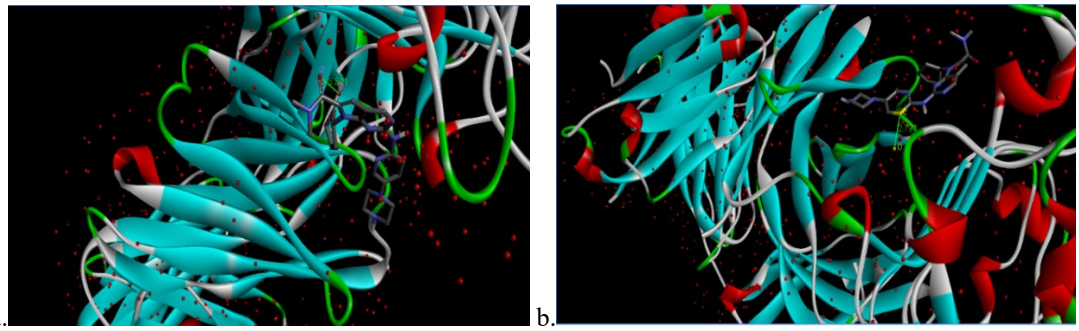

Figure 8: Docked poses of ribociclib with EGFR receptor (PDB ID:3POY)

a. b.

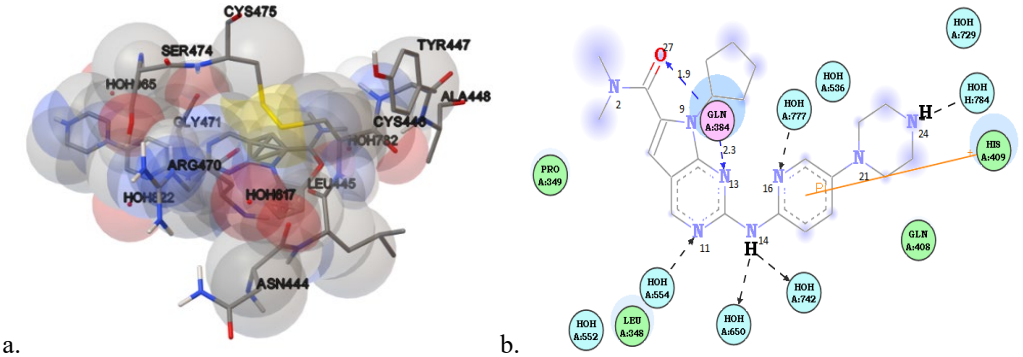

Figure 9: (a) 3D and (b) 2D ligand-protein interaction of ribociclib with 3POY

a. b.

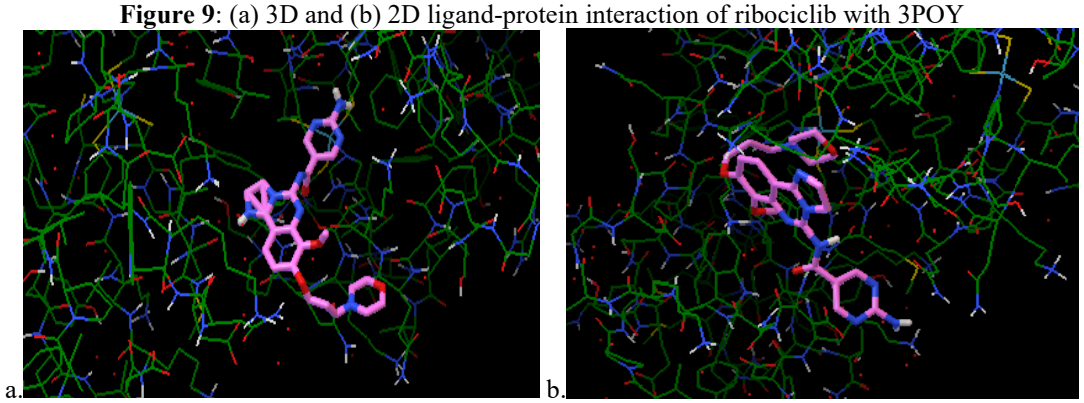

Figure 10: Docking of the drug copanlisib (a) before optimization, (b) after optimization

a. b.

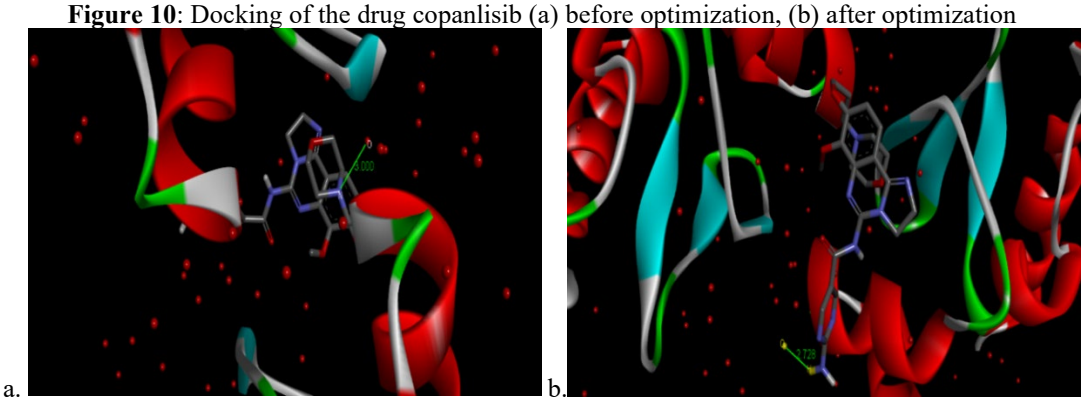

Figure 11: Docked poses of copanlisib with cIAP1 receptor (PDB ID:3M1D)

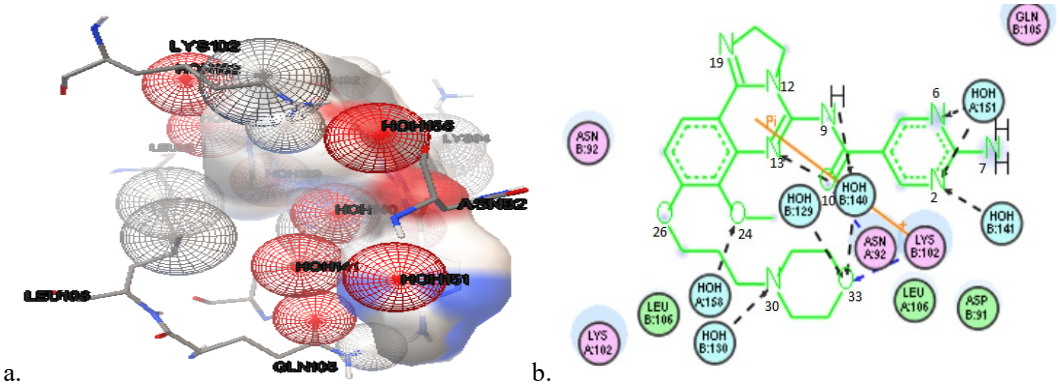

a. b.

Figure 12: (a) 3D and (b) Two-Dimensional ligand-protein interaction of copanlisib with 3M1D

From the docking results of copanlisib, the binding energies of the drug before and after optimization are -11.21 and -14.41 kcal.mol-1 respectively. The docked molecule is bound to the hydrophobic pocket of amino acids viz, LYS 94, ASP 97, ASN 92, GLN 105, GLN 101, LYS 102A, LYS 102B, LEU 106, LEU 90, ASP 91. Atoms N6, N2, N9, 033, N30, and 024 were involved in hydrogen bonding interaction with the water molecule at 2.8, 3.2, 2.2, 2.9, 3.0, and 2.7 Å, respectively (figure 11). LEU 106, LEU 90, ASP 91 involved in Vanderwaals interaction. Pyrimidine ring shows pi interaction with LYS 102 at 4.4 Å. It was revealed that there was an inductive effect. Atom O10 involves hydrogen bond interaction with ASN 92 at 2.9 Å, and O33 involves interaction with LYS 102 at 1.8 Å. Atoms O10 and O33 act as a nucleophile. Due to conjugation, O10 shows more electronic effects than O33. Since the atom O33 is inside the ring, it is more stabilized, and thus, O10 is more reactive.

4. Conclusions

DFT quantum chemical computations employing B3LYP/ 631G basis set was used to optimize two anti-cancer drugs, ribociclib and copanlisib. Reactivity descriptor parameters like electronegativity, softness, hardness, and HOMO-LUMO energies were computed. From the docking studies of ribociclib, atoms O27 and N13 were found to be involved in active site formation with the EGFR receptor protein. Copanlisib showed pi-interaction between the pyrimidine ring. Atom O10 interacts with amino acid ASN 92, atom O33 with LYS 102 and involved in active site formation. From the binding energy values, the energy optimized drug molecules were concluded to be more significant in binding with the receptor. In both the drugs, electrons resonated, and due to the electronic effect, atoms O27 and O10 were evaluated to have non-covalent bond formation since it offers an electron cloud tilt towards GLN 384 and ASN 92 with bond lengths of 1.9 Å and 2.9 Å, respectively. Hence these atoms are reported to be the most reactive atoms based on the high softness values. The ADMET profile of drugs revealed that the drug possess good solubility. According to the BOILED-Egg graph, ribociclib has high passive gastrointestinal absorption while copanlisib has low absorption and limited brain permeability. Predicted toxicity was class five for both anti-cancer drugs. From the insilico investigation, appropriate structural modification of the drugs can establish more potential derivatives of the drugs.

References

[1] Masoudkabir, F., Sarrafzadegan, N., Gotay, C., Ignaszewski, A., Krahn, A. D., Davis, M. K., Mani, A. Cardiovascular disease and cancer: Evidence for shared disease pathways and pharmacologic prevention. Atherosclerosis, 263 (2017) 343–351. doi:10.1016/j.atherosclerosis.2017.06.001

[2] RamdasNayak MBBS MD., Exam Preparatory Manual for Undergraduates-Pathology. Second Edition: 2017.ISBN 978-93-86261-21-2

[3] Sorlie, T., Perou, C. M., Tibshirani, R., Aas, T., Geisler, S., Johnsen, H., Borresen-Dale, A. L. Gene expression patterns of breast carcinomas distinguish tumor subclasses with clinical implications. Proceedings of the National Academy of Sciences, 98(19) (2001) 10869–10874. doi:10.1073/pnas.191367098

[4] Perou, C. M., Sørlie, T., Eisen, M. B., van de Rijn, M., Jeffrey, S. S., Rees, C. A., Botstein, D. Molecular portraits of human breast tumours. Nature, 406(6797) (2000) 747–752. doi:10.1038/35021093

[5] Giancotti, F. G. Deregulation of cell signaling in cancer. FEBS Letters, 588(16), (2014) 2558–2570. doi:10.1016/j.febslet.2014.02.005

[6] Glück, S. Consequences of the Convergence of Multiple Alternate Pathways on the Estrogen Receptor in the Treatment of Metastatic Breast Cancer. Clinical Breast Cancer, 17(2) (2017) 79–90. doi:10.1016/j.clbc.2016.08.004

[7] Dragani, T. A., Castells, A., Kulasingam, V., Diamandis, E. P., Earl, H., Iams, W. T., Schalken, J. A. Major milestones in translational oncology. BMC Medicine, 14(1) (2016). doi:10.1186/s12916-016-0654-y

[8] Supreet Kaur Gill, Ajay Francis Christopher, Vikas Gupta, Parveen Bansal. Emerging role of bioinformatics tools and software in evolution of clinical research. Perspectives in Clinical Research 7(3) (2016) 115-122. DOI: 10.4103/2229-3485.184782

[9] Katsila, T., Spyroulias, G. A., Patrinos, G. P., &Matsoukas, M.-T. Computational approaches in target identification and drug discovery. Computational and Structural Biotechnology Journal, 14 (2016) 177–184. doi:10.1016/j.csbj.2016.04.004

[10] Karim, S., Al-Maghrabi, J. A., Farsi, H. M. A., Al-Sayyad, A. J., Schulten, H.-J., Buhmeida, A., … Al-Qahtani, M. H. Cyclin D1 as a therapeutic target of renal cell carcinoma- a combined transcriptomics, tissue microarray and molecular docking study from the Kingdom of Saudi Arabia. BMC Cancer, 16(S2) (2016) 741. doi:10.1186/s12885-016-2775-2

[11] Hiteshi T, Tanmoy C, Vandana S. A Brief Review on Importance of DFT In Drug Design. Res Med Eng Sci. 7(4) (2019). doi: 10.31031/RMES.2019.07.0006

[12] Ramachandran K. I., DeepaNamboori G., K. Computational Chemistry and Molecular Modeling (2008). doi:10.1007/978-3-540-77304-7

[13] Tsubomura H, Mullikken R S; J. Am. Chem. Soc., 82 (1960) 5966

[14] A Thesis submitted by Mohamed Imran P K. Chemical Reactivity Descriptors from Theoretical Methods for structure-property Evaluation of Small Molecules

[15] Sevvanthi, S., Muthu, S., & Raja, M. Molecular docking, vibrational spectroscopy studies of (RS)-2-(tert-butylamino)-1-(3-chlorophenyl)propan-1-one: A potential adrenaline uptake inhibitor. Journal of Molecular Structure, 1173 (2018) 251–260. doi:10.1016/j.molstruc.2018.07.001

[16] Ramachandran, K. I., G. Deepa, and K. Namboori. (2008) Computational chemistry and molecular modeling: principles and applications. Berlin: Springer. http://site.ebrary.com/id/10284515

[17] Chandrakumar, K., & Pal, S. The Concept of Density Functional Theory Based Descriptors and its Relation with the Reactivity of Molecular Systems: A Semi-Quantitative Study. International Journal of Molecular Sciences, 3(4) (2002) 324–337. doi:10.3390/i3040324

[18] Gross, K. C., & Seybold, P. G. Substituent effects on the physical properties and pKa of aniline. International Journal of Quantum Chemistry, 80(4-5) (2000) 1107–1115. doi:10.1002/1097461x(2000)80:4/5<1107::aid-qua60>3.0.co;2-t

[19] Fukui, K. (1970). Theory of orientation and stereoselection. In: Orientation and Stereoselection. Fortschritte der ChemischenForschung, vol 15/1. Springer, Berlin, Heidelberg. https://doi.org/10.1007/BFb0051113

[20] Fukui K; Science, 1982, 218, 747

[21] Sakthivel, S., Alagesan, T., Muthu, S., Abraham, C. S., & Geetha, E. Quantum mechanical, spectroscopic study (FT-IR and FT - Raman), NBO analysis, HOMO-LUMO, first order hyperpolarizability and docking studies of a non-steroidal anti-inflammatory compound. Journal of Molecular Structure, 1156 (2018) 645–656. doi:10.1016/j.molstruc.2017.12.024

[22] Fukui, K. (1975). Theory of orientation and stereoselection. In: Orientation and Stereoselection. Fortschritte der ChemischenForschung, vol 15/1. Springer, Berlin, Heidelberg

[23] Yang, W., Mortier, W. J. The use of global and local molecular parameters for the analysis of the gas-phase basicity of amines. Journal of the American Chemical Society, 108(19) (1986) 5708–5711. doi:10.1021/ja00279a008

[24] Laurent, A. D., &Jacquemin, D. TD-DFT benchmarks: A review. International Journal of Quantum Chemistry, 113(17) (2013) 2019–2039. doi:10.1002/qua.24438

[25] ACD/ChemSketch, version 2021.1. 1, Advanced Chemistry Development, Inc., Toronto, ON, Canada, www.acdlabs.com, 2021

[26] Hanwell, M. D., Curtis, D. E., Lonie, D. C., Vandermeersch, T., Zurek, E., & Hutchison, G. R. Avogadro: an advanced semantic chemical editor, visualization, and analysis platform. Journal of Cheminformatics, 4(1) (2012)17. doi:10.1186/1758-2946-4-17

[27] G. teVelde, F.M. Bickelhaupt, E.J. Baerends, C. Fonseca Guerra, S.J.A. van Gisbergen, J.G. Snijders and T. Ziegler, Chemistry with ADF, Inc. J ComputChem, 22(2001) 931–967, doi: 10.1002/jcc.1056

[28] Morris, G. M., Huey, R., Lindstrom, W., Sanner, M. F., Belew, R. K., Goodsell, D. S., & Olson, A. J. AutoDock4 and AutoDockTools4: Automated docking with selective receptor flexibility. Journal of Computational Chemistry, 30(16) (2009) 2785–2791. doi:10.1002/jcc.21256

[29] Dassault Systèmes BIOVIA, Discovery Studio Modeling Environment, Release 2017, San Diego: DassaultSystèmes, 2016

[30] Daina, A., Michielin, O., & Zoete, V. SwissADME: a free web tool to evaluate pharmacokinetics, drug-likeness and medicinal chemistry friendliness of small molecules. Scientific Reports, 7(1) (2017). doi:10.1038/srep42717

[31] Banerjee, P., Eckert, A. O., Schrey, A. K., & Preissner, R. ProTox-II: a web server for the prediction of toxicity of chemicals. Nucleic Acids Research, 46(W1) (2018) W257–W263. doi:10.1093/nar/gky318

[32] Thompson, M.A. (2004) Molecular Docking Using ArgusLab, an Efficient Shape-Based Search Algorithm and a Score Scoring Function. ACS Meeting, Philadelphia

[33] Zhurko GA, Zhurko DA. Chemcraft Program, Academic version 1.5, 2004

[34] Gaitonde, Vishwanath; Karmakar, Partha; Trivedi, Ashit (2020). Drug Discovery and Development - New Advances, Molecular Docking in Modern Drug Discovery: Principles and Recent Applications., 10.5772/intechopen.77685(Chapter 3), –. doi:10.5772/intechopen.85991

[35] Hojjat-Farsangi, M. Small-Molecule Inhibitors of the Receptor Tyrosine Kinases: Promising Tools for Targeted Cancer Therapies. International Journal of Molecular Sciences, 15(8) (2014) 13768–13801. doi:10.3390/ijms150813768

[36] Murphy, C. G., & Dickler, M. N. The Role of CDK4/6 Inhibition in Breast Cancer. The Oncologist, 20(5) (2015) 483–490. doi:10.1634/theoncologist.2014-0443

[37] https://go.drugbank.com/drugs/DB12483

[38] Patnaik, A., Appleman, L. J., Tolcher, A. W., Papadopoulos, K. P., Beeram, M., Rasco, D. W., Ramanathan, R. K. First-in-human phase I study of copanlisib (BAY 80-6946), an intravenous pan-class I phosphatidylinositol 3-kinase inhibitor, in patients with advanced solid tumors and non-Hodgkin's lymphomas. Annals of Oncology, 27(10) (2016) 1928–1940. doi:10.1093/annonc/mdw282

[39] Eltantawy, A., Vallejos, X., Sebea, E., & Evans, K. Copanlisib: An Intravenous Phosphatidylinositol 3-Kinase (PI3K) Inhibitor for the Treatment of Relapsed Follicular Lymphoma. Annals of Pharmacotherapy, 53(9) (2019) 954–958. doi:10.1177/1060028019833992

[40] M. Dreyling, D. Cunningham, K. Bouabdallah, S. Assouline, E. V. den Neste, U. Vitolo, M. Giurescu, S. Mappa, J. Grunert, B. H. Childs and F. Morschhauser, Blood, 124 (2014) 1701. doi:10.1182/blood.V124.21.1701.1701

[41] Salim Meeran I ,Baskar V., Syed Tajudeen S., Shabeer T. K..Design, ADME Profiling, and Molecular Docking Simulation of New Isoniazid-Schiff Base Analogs as MtKasB Inhibitors. Asian Journal of Research in Chemistry and Pharmaceutical Sciences, 6(1) (2018) 20-34

[42] Chandrakumar, K., & Pal, S. The Concept of Density Functional Theory Based Descriptors and its Relation with the Reactivity of Molecular Systems: A Semi-Quantitative Study. International Journal of Molecular Sciences, 3(4) (2002) 324–337. doi:10.3390/i3040324

[43] Gross, K. C., & Seybold, P. G. Substituent effects on the physical properties and pKa of aniline. International Journal of Quantum Chemistry, 80(4-5) (2000) 1107–1115. doi:10.1002/1097-461x(2000)80:4/5<1107::aid-qua60>3.0.co;2-t

[44] Sakthivel, S., Alagesan, T., Muthu, S., Abraham, C. S., &Geetha, E. Quantum mechanical, spectroscopic study (FT-IR and FT - Raman), NBO analysis, HOMO-LUMO, first order hyperpolarizability and docking studies of a non-steroidal anti-inflammatory compound. Journal of Molecular Structure,

1156 (2018) 645–656. doi:10.1016/j.molstruc.2017.12.024

[45] Muthu, S., Elamurugu Porchelvi, E., Karabacak, M., Asiri, A. M., &Swathi, S. S. Synthesis, structure, spectroscopic studies (FT-IR, FT-Raman and UV), normal coordinate, NBO and NLO analysis of salicylaldehyde p-chlorophenylthiosemicarbazone. Journal of Molecular Structure, 1081 (2015) 400–412. doi:10.1016/j.molstruc.2014.10.024

[46] Kuruvilla, T. K., Muthu, S., Prasana, J. C., George, J., &Sevvanthi, S. Spectroscopic (FT-IR, FT-Raman), quantum mechanical and docking studies on methyl[(3S)-3-(naphthalen-1-yloxy)-3-(thiophen-2-yl)propyl]amine. Journal of Molecular Structure, 1175 (2019) 163–174. doi:10.1016/j.molstruc.2018.07.097

[47] Tüzün, B.. Investigation of pyrazoly derivatives schiff base ligands and their metal complexes used as anti-cancer drug. Spectrochimica Acta Part A: Molecular and Biomolecular Spectroscopy, 227 (2020) 117663. doi:10.1016/j.saa.2019.117663

[48] Bytyqi-Damoni, A., Kestane, A., Taslimi, P., Tuzun, B., Zengin, M., Bilgicli, H. G., & Gulcin, İ. Novel carvacrol based new oxypropanolamine derivatives: Design, synthesis, characterization, biological evaluation, and molecular docking studies. Journal of Molecular Structure (2019), 127297. doi:10.1016/j.molstruc.2019.127297

[49] Genc Bilgicli, H., Taslimi, P., Akyuz, B., Tuzun, B., & Gulcin, İ. Synthesis, characterization, biological evaluation, and molecular docking studies of some piperonyl-based 4-thiazolidinone derivatives. Archiv Der Pharmazie, (2019) e1900304. doi:10.1002/ardp.201900304

[50] Roskoski, R. Small molecule inhibitors targeting the EGFR/ErbB family of protein-tyrosine kinases in human cancers. Pharmacological Research. 139 (2019) 395–411. doi:10.1016/j.phrs.2018.11.014.

[51] Eckelman, B. P., Drag, M., Snipas, S. J., & Salvesen, G. S. The mechanism of peptide-binding specificity of IAP BIR domains. Cell Death & Differentiation, 15(5) (2008) 920–928. doi:10.1038/cdd.2008.6

[52] Ma, O., Cai, W.-W., Zender, L., Dayaram, T., Shen, J., Herron, A. J., … Donehower, L. A. MMP13, Birc2 (cIAP1), and Birc3 (cIAP2), Amplified on Chromosome 9, Collaborate with p53 Deficiency in Mouse Osteosarcoma Progression. Cancer Research, 69(6) (2009) 2559–2567. doi:10.1158/0008-5472.can-08-2929

[53] Jung, S. A., Park, Y.-M., Hong, S.-W., Moon, J.-H., Shin, J.-S., Lee, H.-R., Kim, T. Cellular Inhibitor of Apoptosis Protein 1 (cIAP1) Stability Contributes to YM155 Resistance in Human Gastric Cancer Cells. Journal of Biological Chemistry, 290(16) (2015) 9974–9985. doi:10.1074/jbc.m114.600874

[54] Yang, C., Wang, H., Zhang, B., Chen, Y., Zhang, Y., Sun, X., Qin, S. LCL161 increases paclitaxel-induced apoptosis by degrading cIAP1 and cIAP2 in NSCLC. Journal of Experimental & Clinical Cancer Research, 35(1) (2016). doi:10.1186/s13046-016-0435-7

[55] Cartier, J., Berthelet, J., Marivin, A., Gemble, S., Edmond, V., Plenchette, S., Dubrez, L. Cellular Inhibitor of Apoptosis Protein-1 (cIAP1) Can Regulate E2F1 Transcription Factor-mediated Control of Cyclin Transcription. Journal of Biological Chemistry, 286(30) (2011) 26406–26417. doi:10.1074/jbc.m110.191239.